CrossMark

Non-destructive Investigation of Paintings on Canvas by Continuous Wave Terahertz Imaging and Flash Thermography

Hai Zhang[1] · Stefano Sfarra[2,3] · Karan Saluja[4] · Jeroen Peeters[5] · Julien Fleuret[1] · Yuxia Duan[6] · Henrique Fernandes[7] · Nicolas Avdelidis[8] · Clemente Ibarra-Castanedo[1] · Xavier Maldague[1]

Abstract Terahertz (THz) imaging is increasingly used in the cultural heritage field. In particular, continuous wave (CW) and low frequency THz is attracting more attention. The first application of the THz technique inherent to the cultural heritage field dates back 10 years ago. Since 2006, tangible improvements have been conducted in the refinement of the technique, with the aim to produce clear maps useful for any art restorer. In this paper, a CW THz (0.1 THz) imaging system was used to inspect paintings on canvas both in reflection and in transmission modes. In particular, two paintings were analyzed: in the first one, similar materials and painting execution of the original artwork were used, while in the second one, the canvas layer is slightly different. Flash thermography was used herein together with the THz method in order to observe the differences in results for the textile support materials. A possible application of this method for the detection of artwork forgery requires some parameterization and analysis of various materials or thickness influence which will be addressed in a future study. In this work, advanced image processing techniques including principal component thermography (PCT) and partial least squares thermography (PLST) were used to process the infrared data. Finally, a comparison of CW THz and thermographic results was conducted.

✉ Hai Zhang
hai.zhang.1@ulaval.ca

[1] Department of Electrical and Computer Engineering, Computer Vision and Systems Laboratory (CVSL), Laval University, 1065 av. de la Médecine, Quebec G1V 0A6, Canada

[2] Department of Industrial and Information Engineering and Economics, Las.E.R. Laboratory, University of L'Aquila, Piazzale E. Pontieri no. 1, 67100 Roio Poggio, AQ, Italy

[3] Tomsk Polytechnic University, Savinykh St., 7, Tomsk, Russia 634028

[4] Department of Electrical and Electronics Engineering, Birla Institute of Technology and Science, Pilani, Rajasthan 333031, India

[5] Department of Electromechanical Engineering, Optical Metrology, 3D Design and Mechanics Laboratory (Op3Mech), University of Antwerp, Groenenborgerlaan 171, 2020 Antwerp, Belgium

[6] School of Physics and Electronics, Central South University, 932 Lushan South Road, Changsha 410083, China

[7] Department of Computer Science, Federal University of Uberlandia, 2121 Avenida Joao Naves de Avila, Uberlandia 38400-902, Brazil

[8] Materials Science & Engineering Department, NDT Laboratory, School of Chemical Engineering, National Technical University of Athens, Zografou Campus, 157 80 Athens, Greece

Keywords Terahertz imagery · Continuous wave · Flash thermography · Painting on canvas · Nondestructive testing

1 Introduction

The use of terahertz (THz) technology has been magnificently described in a book recently published [54]. Among the various applications that are possible with THz, its use in the cultural heritage (CH) field is attracting increasing attention. Recently, different applications have been introduced in the scientific panorama by eminent research groups. In particular, the attention was focused on panel paintings, taking into account both the nature of the defects and the type of the materials which, usually, constitute them. In the authors' opinion, it is important to first briefly summarize the salient works already carried out in this research field for the sake of clar-

ity for the reader and, secondly, to introduce the advantages that an integrated approach, *e.g.*, with infrared thermography (IRT) can produce in terms of additional information for comparison purposes.

In 2015, Kock Dandolo et al. applied THz—time domain imaging (TDI) for non-destructive visualization of a hidden painting and other subsurface composition layers of a seventeenth century panel painting belonging to the National Gallery of Denmark. Plan-type and cross-sectional scans achieved by THz have been compared with X-ray images, thus helping in the understanding of the advantages and disadvantages of the technique for art diagnostic purposes [12]. Simultaneously, Koch Dandolo et al. also explored and imaged subsurface features of panel paintings through gilded finishes with THz-TDI. Subsurface layers of three gilded panel paintings (two contemporary tempera panel replicas and one fourteenth-century icon) have been successfully imaged behind gold finishes with THz-TDI [36]. Instead, Abraham et al. revealed buried layer information such as a graphite handmade sketch covered by several layers of paint. In addition, taking advantage of the pulsed THz emission, the authors demonstrated that it was also possible to evaluate the variations of the painting thickness [2]. Labaune et al. applied THz-TDI on papyrus texts, including images of hidden papyri. Inks for modern papyrus specimens were prepared using the historical binder, Arabic gum, and two common pigments used to write ancient texts, carbon black and red ochre. Temporal analysis of the signals provides the depths of the layers, and their frequency spectra give information about the inks [39]. Abraham and Fukunaga employed onsite THz radiation for the analysis of museum artifacts related to art conservation science. The authors used two complementary portable THz imaging devices which have been employed at the Tokyo National Museum (Japan) and at the Museum of Aquitaine (France). A Japanese panel screen, African fetish figures, and a nearly 3500-year-old sealed Egyptian jar were imaged with THz waves, revealing their internal structures [1]. In 2016, Fukunaga et al. applied THz pulsed TDI technique and near-infrared observation to investigate an oil painting on canvas by Pablo Picasso. The multilayer structure was clearly observed in a cross-sectional image by THz pulsed TDI, and particular Cubism style lines were revealed under newly painted areas by near-infrared imaging [21]. One year before, Picollo et al. probed two masterpieces by Giotto di Bondone and by Masaccio. Data acquired at a noninvasive level on panel paintings provided useful information on their internal structures. In addition, a first attempt in the understanding of the chemical composition of the artworks was scientifically validated [51]. The combination THz—chemical characterization was also implemented three years before by Trafela et al. In their paper, THz spectroscopy in the time domain was explored in combination with multivariate data analysis

for quantitative determination of chemical and mechanical properties of historic paper, such as lignin content, tensile strength, and ash content. Using partial least squares (PLS) regression, it was shown that quantitative prediction of the material properties is possible, which indicates the potential of THz spectroscopy for chemical characterization of complex organic materials of natural origin [69]. A comparative study between ultraviolet, visible, infrared (by using the well-known PPT technique) and THz spectra was conducted in the same year by Bendada et al. [8]. The work was based on non-simultaneous multi-spectral inspections of a panel painting sample, using a set of detectors covering from the ultraviolet to the THz spectra. The THz technique provided more information regarding the wood support (rings), as well as an indication of a sub-superficial inclusion of foreign material. Another comparative study between shearography and THz imaging for evaluating a wooden panel painting was reported by Groves et al. [26]. Gallerano et al. have investigated hidden paintings since 2008. The colleagues also calculated the refractive indexes of artwork materials, as well as the ability of distinguishing pigments via the THz technique [22].

The exponential growth in the use of THz applications in the NDT&E research field is due to the fact that the THz region (from 0.1 to 10 THz in terms of frequencies) is an area of convergence between the electronics and the photonics fields in the electromagnetic spectrum. Among the advantages that can be underlined regarding the THz radiation, it is possible to remember that it can penetrate through a wide variety of dielectric materials (*e.g.*, fabric, paper, plastic, leather, and wood), it is non-ionizing and has minimal effects on the human body (as opposed to X-ray radiation), it demonstrates a very large absorption when meeting water aggregates or humid materials while it is highly reflected when it hits metal surfaces [4,5]. Concerning the disadvantages with respect to, *e.g.*, near-infrared reflectography/transmittography technique [9], the detecting of THz signals is difficult because blackbody radiation at room temperatures is strong at THz frequencies. Another concern for THz imaging is the atmospheric transmission. The atmospheric attenuation of the THz domain is higher than in the other spectral regions, such as infrared and visible-light regions [49]. This requires that THz imaging should be short-range when compared to imaging in the other modalities. Another problem is the selection of appropriate optics in imaging systems. Generally, lenses are not used so widely in the THz regime because of lack of convenient materials and anti-reflection coatings functioning over a wide range of frequencies [40]. Difficulties in the construction of advanced lenses are associated with one of the most important limitations of THz systems, which is the measurement resolution. Despite the increasing number of pixels in cameras, THz solutions are as limited by the diffraction phenomenon as are any other imaging systems. An absolute upper performance

limit linked to the laws of physics is controlled by the sensor size working f-number of the lens and the wavelength of light that passes through the lens [42]. In the diffraction-limited case, frequency determines resolution [24]. To improve the signal-to-noise ratio (SNR), THz images can be obtained by mechanically scanning the object—pixel by pixel—with the use of a coherent source. However, this solution may be applied only for static objects, and it is difficult to export the apparatus in situ.

In this work, the authors studied the ability of a continuous-wave (CW) THz source for the detection of the nature of different canvas supports beneath oil paintings. Since the canvas layers can sometimes be doubled and of different nature in the same painting, what is visible from the rear side does not correspond to the reality. It follows the definition of art forgery, *e.g.*, a process of creating a piece of art by copying an existing piece or by mimicking the style of another artist with the use of certain materials to falsely attribute and (or) date works of art [25]. Forgery recognition and attribution processes require a detailed knowledge of the history and the work of a particular artist, materials available at the time when the artwork was allegedly created, as well as the manner of creation used by the artists. At the same time, forgers continue to enhance their skills in mimicking styles, using old canvas as skins of a core made by a different product (which have the intent to reach the right thickness). To counteract this, art experts rely heavily on various scientific methods now available [11]. Explained above regarding the main disadvantages of the X-ray technique, the neutron activation is used less frequently than infrared in order to reveal details of composition hidden by the top layers of the painting under investigation. The primary reason for this is the necessity to use a nuclear reactor as the source of neutrons, which significantly limits the availability of the method because of cost and physical location of the reactor; another reason is the residual radioactivity of paintings [37]. Additional options may be the use of acoustic analysis [23] or ground penetrating radar technique [13]. However, acoustic analysis remains today somewhat exotic for the field of analysis of art. The main limiting factors are the speed of raster scanning and difficulties with the fine tuning of the setup. Often the successful operation of the device requires that a qualified specialist be involved. The number of publications on this subject is relatively limited, and the scope of research mostly includes mural and panel paintings (not paintings on canvas) [44,47,64]. When using the ground penetrating radar technique, interpretation of radargrams is generally non-intuitive to the novice and, in the CH field, it is usually used for thick objects, such as mural paintings [52] or historical floors [56] and not for thin objects, such as paintings on canvas, due to the operation frequency. The use of IRT can be a valid choice in order to support the THz imaging in the artwork inspection and in the distinction between genuine or fake weaving in paintings on canvas. Indeed, it is a non-contact, non-intrusive and non-invasive method which permits a series of advanced post-processing operations to seeing the unseen [16,45,72], *e.g.*, canvas cuspings [58], underdrawings [32], covered signatures [61], sub-superficial defects [63] and repairs [57], wood analysis [31], the rising damp effect [68], inclusions of heterogeneous materials [17,41,62], porosity [73,74,76] and fiber orientation [19]. In the present research work the authors demonstrate how the use of principal component thermography (PCT) [53] and partial least square thermography [43] techniques applied under flash thermography conditions can help to retrieve some important differences between a sample constructed following the art master rules and a fraudulent work of art, when the results are compared with the THz imaging observations.

2 Description of the Samples

The canvas prototypes used in this paper were composed of hybrid textile supports, with different textile fibers. Once mounted on a wooden frame, the prototypes were painted using the original execution technique inherent to the painting selected as representative samples to be duplicated. The original artwork is an oil painting on canvas produced in 1871 by James Abbott McNeill Whistler, titled *Portrait of the Painter's Mother* (Fig. 1) [6,14,20,67].

The scale drawings were, therefore, reproduced on two different hybrid fabric supports (Fig. 2). Regarding the preparation of the specimens, textile fibers which exhibit adequate mechanical characteristics for conservation purposes were

Fig. 1 James Abbott McNeill Whistler, Arrangement in *Grey* and *Black*, No. 1: *Portrait of the Painter's Mother*, 1871, oil on canvas, 144.3 cm × 162.4 cm, Musée d'Orsay, Paris

Fig. 2 The photographs of the paintings on canvas: **a** the canvas A, **b** the canvas B, **c** the textile support made from hemp and nettle, **d** the textile support made from flax and juniper
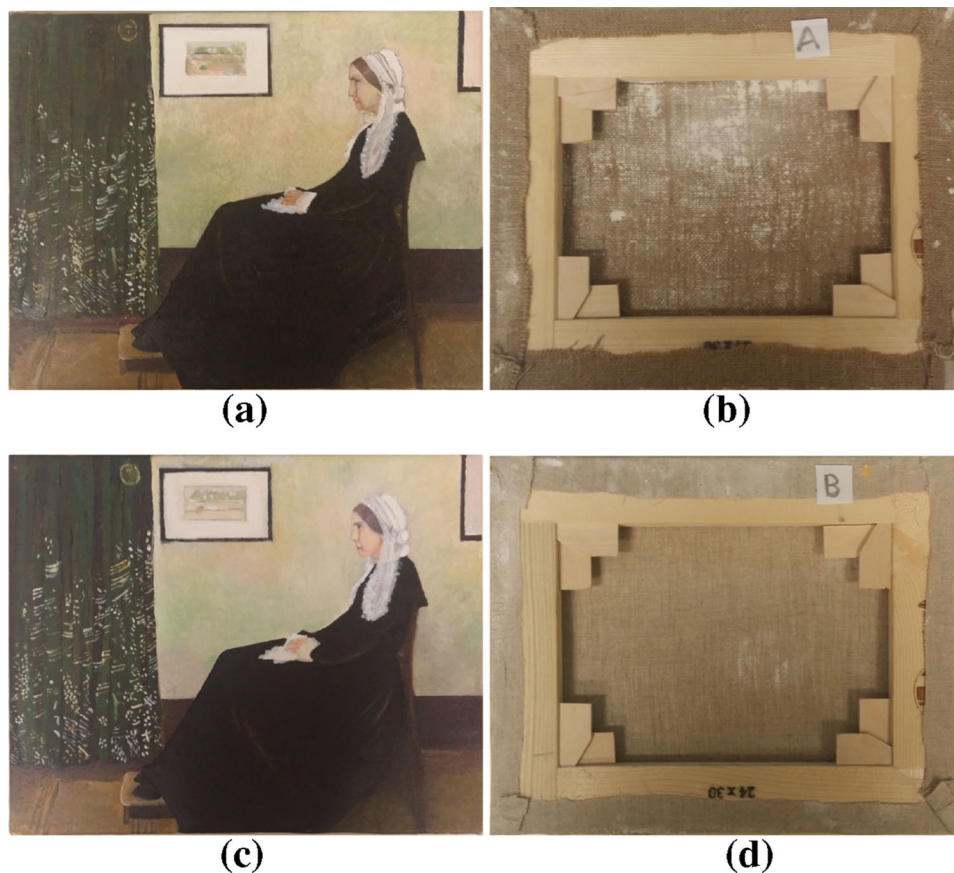
selected. The weft-insertion usually recommended is 12 yarns (weft) : 12 yarns (warp) cm^2. The final dimensions of the specimens are 24 cm × 30 cm. The textile support of canvas A was made from hemp and nettle, while the textile support of canvas B was made from flax and juniper. The material of canvas A is close to that of the original artwork, while in painting B, the force used on the paint brush was almost double with respect to the painting B. The method to paint by pressing on the canvas through the paint brush is the opposite used by the art masters, in general.

3 Methodology

3.1 Continuous Wave Terahertz Imaging

The electromagnetic waves range inherent to THz spectroscopy is located between 0.1 and 10 THz. THz wave generation is a challenge because the THz range is located at the boundary of electronics (based on the motion of electrons) and the photonics (based on the atomic transitions of electrons) modes of EM wave generation [3]. However, the development of photonics and electronics in recent years has enabled the compact yet sophisticated THz imaging systems [15]. The principles of continuous wave (CW) imaging has

been known for several decades [27,46]. Pulse imaging can provide depth, frequency-domain or time-domain information of the object, while CW imaging can only yield intensity data using a fixed frequency source and a single detector [28]. However, in THz imaging, a CW imaging system is compact, simple and relatively low-cost without a pump-probe system. Simultaneously, the complexity of the optics involved can be greatly reduced [65]. A recent THz time-domain system uses a shaker-technique to reduce measurement time, so the total observation time depends on scanning itself. Therefore, both pulse and CW THz systems can provide fast scanning. Regarding scientific research, simplicity is the main advantage of CW THz while the key advantage of pulse THz is flexibility, in which all the information is recorded within a single measurement to be processed in order to acquire the needed information for different applications. Since the frequency spectrum of CW THz is narrow, a large F-number Fresnel lens can be used to increase the resolution by focusing onto a spot [33].

In order to introduce the reader to the "result analysis" section it is important to describe the main physical concepts at the base of the THz method, as well as the experimental set up used to record the data. Usually, materials have different reflection and absorption coefficients for THz radiation, *e.g.*, metals are better reflectors, polar liquids such as

Fig. 3 CW sub-THz imaging system: **a** schematic set-up in reflection mode, **b** schematic set-up in transmission mode, **c** experimental set-up in reflection mode, **d** experimental set-up in transmission mode
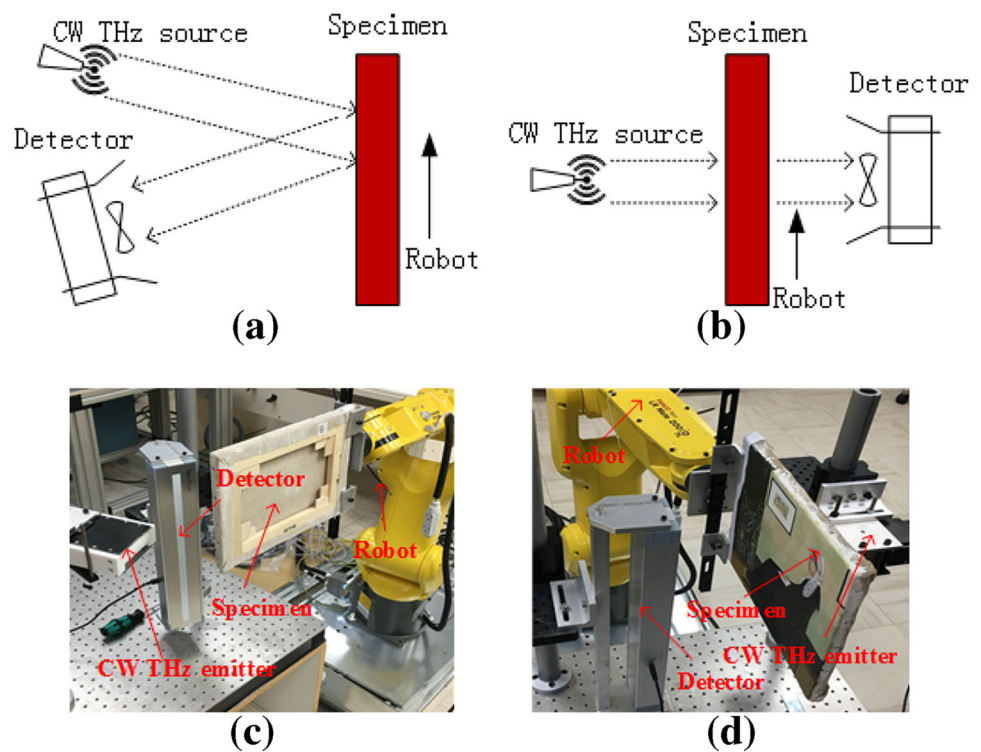
water are excellent absorbers, and anisotropic materials such as composites have variable reflectance relative to the fibre direction. The THz refractive indices and absorption coefficients are related to the material's structure and properties. The Claausius–Mossotti equation (Eq. 1) [34] is usually used to calculate the refractive indices, which links the dielectric constant ε to the microscopic polarizability P,

$$\frac{\varepsilon - 1}{\varepsilon + 2} = \frac{4\pi}{3} N_A \frac{\rho}{M} P \tag{1}$$

where N_A is Avogadro's number, ρ is the mass density, and M is the molecular weight.

The model developed by Schlömann [55] and Strom [66] is usually used to calculate the absorption coefficients. The model explains far-infrared absorption in amorphous materials in terms of disorder-induced coupling of radiation into the acoustic photon modes [48].

CW THz wave propagations in uniform solid materials is linear, and the transmission intensity can fit Beer's Law very well. It is known that spruce absorption correlates with its density in the THz range, and this can be used for density mapping [35]. The derived CW THz absorption coefficient of various timbers can be obtained as follows [50]:

$$\frac{\alpha/cm^{-1}}{\rho/gcm^{-3}} \approx 4.69 \tag{2}$$

where, α is the absorption coefficient at 0.1 THz and ρ is the material density.

The system employed in this paper utilizes IMPAct ionization Transit Time (IMPATT) diodes [10,38,70] to exploit 0.1 THz (sub-THz) CW imaging. The system consists of a detector (TeraSense Linear-1024), a robot (Fanuc LR Mate 200iD 7L), and a CW THz emitter (TeraSense TS 1603). The detector has a spectral range of 40 GHz–0.7 THz and a frame rate of 8.2 fps. The pixel size of the detector is 1.5 mm × 1.5 mm, and the number of pixels is 1024 (256 × 4). The CW THz emitter has an optimized frequency of 0.1 THz and 1 µs rise/fall time (TTL Modulation). The emitted radiation beam is expanded to exploit the detector ability of detecting radiation along a line composed of 256 pixels, which reduces scanning time. The imaging capability of the system is 6 mm (4 pixels) in width and 384 mm (256 pixels) in height. The central region of the detected images (5 mm in width) was selected as the step scanning resolution, and the sample moving speed was set to 5 mm/s. The distance between the sample and the THz emitter was ∼10 cm, which was the same as the distance between the sample and the THz sensor. Figure 3a, c show the reflection mode configuration, in which the CW source and the detector were placed in front of the painting layer. Figure 3b, d show the transmission mode configuration, in which the specimen was placed between the CW source and the detector.

Fig. 4 PT set-up using flash: **a** schematic set-up, **b** experimental set-up

(a)   **(b)**
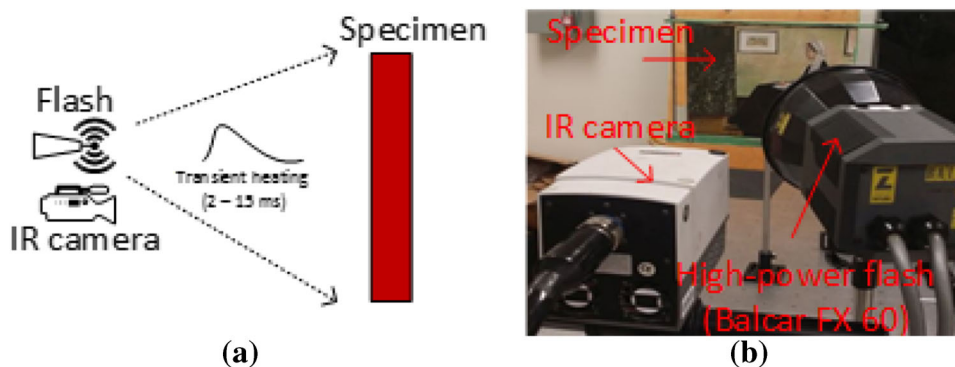
3.2 Flash Thermography

In this paper, flash thermography was used to integrate the CW THz results. In flash thermography, photographic flashes are used to produce a heat pulse (transient pulse) on the specimen surface. Heat transmits through the specimen up to the subsurface, by conduction, and then returns to the specimen surface. As time elapses, the surface temperature decreases uniformly for a specimen without internal flaws. On the contrary, subsurface discontinuities act as resistances to heat flow that change the diffusion rate by producing irregular temperature patterns at the surface. These patterns may be detected with an IR camera; only $\triangle T$ of mK are needed when modern thermal imaging equipment are used [30].

The Fourier equation for the propagation of a Dirac heat pulse in a semi-infinite isotropic solid by diffusion is [7]:

$$T(z, t) = T_0 + \frac{Q}{\sqrt{k\rho c_p \pi t}} e\left(-\frac{z^2}{4\alpha t}\right) \tag{3}$$

where, $Q[J/m^2]$ is the energy absorbed by the surface and $T_0[K]$ is the initial temperature.

A Dirac heat pulse is composed of periodic waves at all frequencies and amplitudes. A photographic flash provides an approximately square-shaped heat pulse, which can be considered a convenient approximation. Therefore, the signal can be decomposed into periodic waves at several frequencies. The shorter the pulse, the broader the range of frequencies [30].

Figure 4 shows the schematic and experimental set-up for PT in which both a Balcar FX 60 (6.4 KJ, 2 ms duration) photographic flash and a mid-wave IR camera (FLIR Phoenix, InSb, 3–5 μm, 640 × 512 pixels) was used. The cooling time was equal to ∼3 s (300 frames) and a frame rate of ∼88 fps was selected by considering the thickness of the material to be inspected. In particular, only one flash was used in order to minimize the effect of an overheating on the paint surface which is a concern for any restorer. Although this procedure can create a non-uniform heating on the surface, this effect can be minimized by applying advanced algorithms to the raw data as explained in the following.

3.3 Image Processing Techniques

In this paper, contrast optimization and median filter were performed in CW THz imaging, while recursive median filter (RMF) and cold image subtraction (CIS) were performed prior to the application of principal component thermography (PCT) and partial least squares thermography (PLST) techniques to the raw thermograms.

CIS decreases the impact of fixed artefacts into thermographic images. These may include reflections from the surrounding area, such as remaining heat from the lamps or reflections from the camera, which appear during the image recording. Because such artefacts do not change, either before heating when the sample is cold or during the process of acquisition, the cold image or the average of a few cold images can be subtracted from the whole sequence [75].

3.3.1 Principal Component Thermography

Principal component thermography (PCT) extracts image features and reduces undesirable signals. It relies on singular value decomposition (SVD), which extracts spatial and temporal data from a matrix in a compact manner by projecting original data onto a system of orthogonal components known as empirical orthogonal functions (EOF). The first EOF will represent the most important characteristic variability of the data; the second EOF will contain the second most important variability, and so on. Usually, original data can be adequately represented with only a few EOFs. Typically, an infrared sequence of 1000 images can be replaced by 10 or fewer EOF [18]. More information regarding the PCT technique can be found in [53].

3.3.2 Partial Least Squares Thermography

Based on a statistical correlation method, partial least squares thermography (PLST) has been recently introduced as a

Fig. 5 CW THz results: **a** painting on canvas A in reflection mode, **b** canvas A in transmission mode, **c** painting on canvas B in reflection mode, **d** canvas B in transmission mode
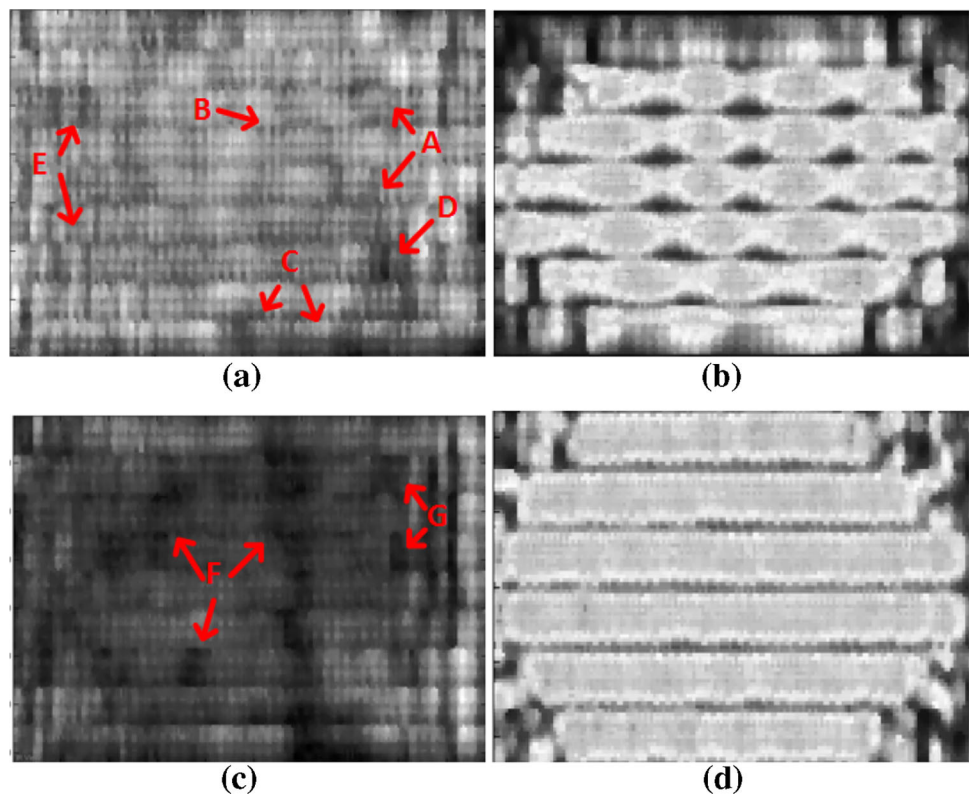
technique for the treatment of thermographic images. PLST computes loading P and score T vectors that are correlated to the predicted block Y (as in maximum redundancy analysis), while describing a large amount of the variation in the predictor matrix X (as in principal component regression). Matrix X corresponds to the surface temperature matrix obtained upon PT inspection, while Y is defined by the observation time of the thermographic acquisition. The partial least squares (PLS) model is achieved by decomposing X and Y into a combination of loadings P and Q (formed by orthogonal vectors), scores T and U (the projections of the loading vectors associated with the singular values) and residuals E and F. Mathematically, the PLS model is expressed as:

$$X = T P^{'} + E \tag{4}$$

$$Y = U Q^{'} + F \tag{5}$$

In order to perform the decomposition of the thermal sequence matrix, it is necessary to select the appropriate number of PLS components. More information regarding the PLST technique can be found in [43].

4 Result Analysis

Figure 5 shows the CW THz results. In order to record the data, the robot was used to move the specimen, continuously and horizontally, with the aim of acquiring a series of narrow

images. The images recorded by the sensor, with a size of 5 mm in width, were used to compose a wide image. Because the samples have a large size in height with respect to potentiality of the system, several scans were carried out along horizontal lines to build the final THz image. The image processing was performed using Python and Matlab scripts.

In reflection mode (Fig. 5a, c), some anomalous signals can be distinguished. They are indicated by arrows and explained in-depth in the following, while in transmission mode (Fig. 5b, d), the results show a periodic trend which is correlated to the wavelength of the radiation. The crossed fibers of the canvas can act as a reflective mesh, thus causing interference patterns depending on the different path length from source to detector. The canvas A (Fig. 5a) indicates a more significant reflectance for THz radiation than the canvas B (Fig. 5c). On the contrary, the canvas B (Fig. 5d) manifests a more significant absorbency for THz radiation than the canvas A (Fig. 5b). These opposite phenomena were caused by the intrinsic characteristics of the supports, which have different absorptivities and reflectivities. In particular, the textile support made from hemp and nettle shows a configuration of spots alternating with high-absorption areas at specific frequency. Instead, the textile support made from flax and juniper displayed a more homogeneous behavior along the inspected lines. It should be noted that the thickness of the canvas supports (Fig. 2b, d) is the same, although in forgery the rear side may not match with the real support. In prac-
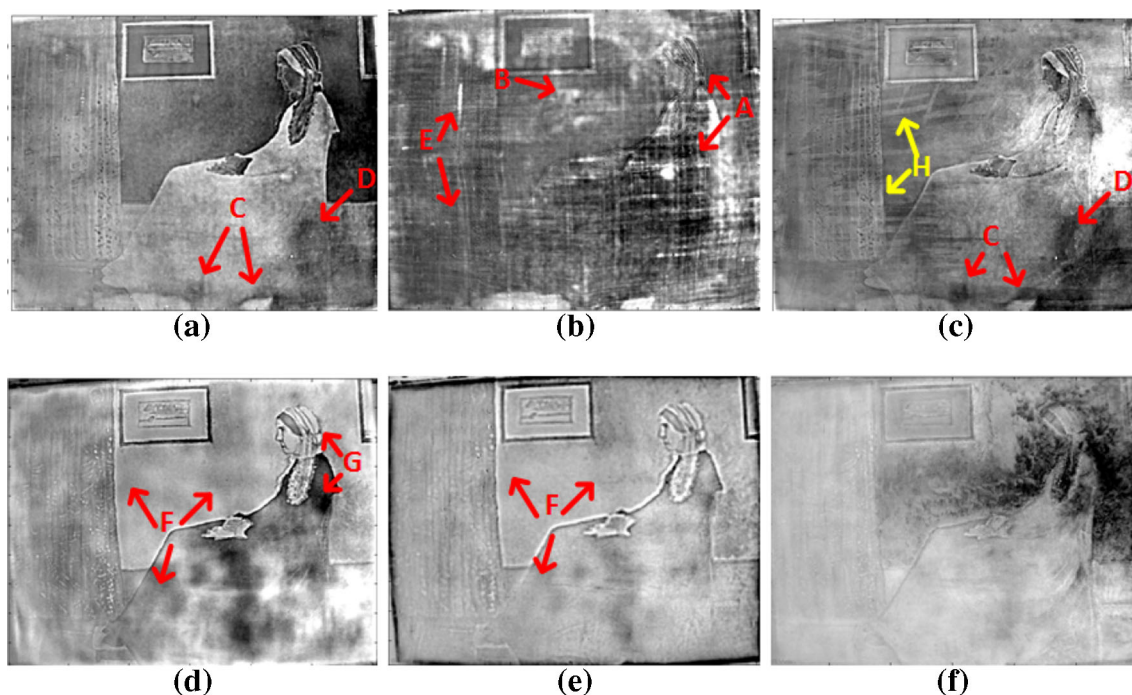
Fig. 6 PCT results: **a** painting A: EOF 02, **b** painting A: EOF 03, **c** painting A: EOF 04, **d** painting B: EOF 02, **e** painting B: EOF 03, **f** paint B: EOF 04

tice, a visual inspection or a simple microscope may not be enough in order to discriminate between a real object or a copy. The results shown herein are greatly significant for distinguishing various materials of similar (but not identical) nature. On one hand, it is obvious that the painted surface does not contribute solely to the discrimination between similar (but not identical) objects. On the other hand, this method could be potentially combined with the classical chemical analyses performed on cross-sections after a micro-sampling procedure [59, 61, 68] in order to discriminate between real or fraudulent artworks. The integration of methods proposed herein, at least when used in reflection mode, is also suited for in situ inspections if a movement off site, *e.g.*, the museum, is not admissible for microclimatic problems.

As mentioned above, some signals not correlated between the paintings can be retrieved. In particular, it seems that a vertical (dark) stripe can be visualized in the canvas B (defect F - on the right). It can be linked to the force used on the paint brush which closed more of the pores between two consecutive fibers. Flash thermography was used to integrate the THz results. Specifically, a part of the features of the woman on painting A was detected. The features A indicate her head and arm in both THz and PCT results. An anomalous signal is marked by the letter B. It is detected more clearly in Fig. 6b. Additional irregularities in the signal variation are present near the feet of the woman as indicated by the letter C in Fig. 5a. They were also detected in Fig. 6a, c. The defect D was also clearly detected both in the THz (Fig. 5a) and PCT

results (Fig. 6c), while the defect E indicates a poor fiber impregnation problem (Fig. 5a, b). These anomalies are not detectable to the naked eye and can be verified by the PCT technique. Interestingly, the warp and weft of the fibers are partially visible after the PCT image processing in Fig. 6c (see the anomaly H indicated by arrows). The latter is not detectable in the same EOF (EOF 04) shown in Fig. 6f, and inherent to the canvas B.

In the THz result (Fig. 5c) linked to the painting on canvas B, the hidden defect F was clearly detected. The same defect was also detected in PCT results shown in Fig. 6d, e. The letter G indicates another signal variation partially located on the head of the woman. This may suggest the presence of a hidden defect corresponding to the position of the woman's head, which may be located at a deeper depth. A longer cooling time during the IRT inspection may contribute to detecting this defect, which presumably is inherent to a thicker point of plaster applied beneath the paint layer (Fig. 2b, d).

Flash thermography is able to provide information concerning the defect depth as studied in [29]. However, the series of the PLST results in Fig. 7, i.e., from Loading 01 to Loading 03 show the images through the increase of depth sounded, in both cases. PLST detected fewer anomalies with respect to the THz and PCT techniques. The signal variation H shows the alignment of the fibers. (Fig. 7b). This may explain the reason why it cannot be detected by THz. In fact, the limit imposed by the wavelength (0.1 THz) plays an important role. On the contrary, the defects B and E were
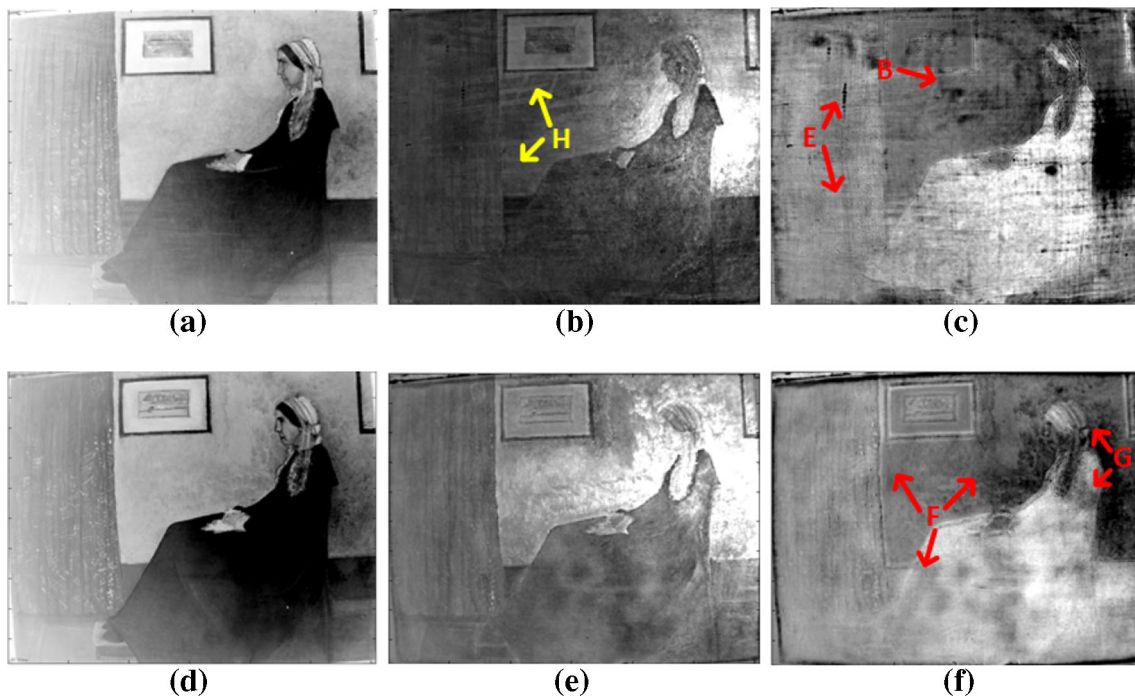
Fig. 7 PLST results: **a** painting A: Loading 01, **b** painting A: Loading 02, **c** painting A: Loading 03, **d** painting B: Loading 01, **e** painting B: Loading 02, **f** paint B: Loading 03

detected at deeper depths as shown in Fig. 7c. The defect F which appears as a vertical stripe on the right side, was confirmed also in this case. It is indeed present in the THz result (Fig. 3c) and in the PCT result (Fig. 6d).

THz and IRT results indicate different sub-superficial anomalies which can be used to discriminate regarding the technical execution, and the modality of application of the materials. Interestingly, in PLST image processing, the Loading 02 in both cases (Fig. 7b, e) isolates the non-homogeneous heating provided by the right lamp (Fig. 4b) into itself. The reader can notice the bright area on the body of the woman. Both the PCT and PLST techniques were not able to retrieve the direction of the fibers for the canvas B. This is an important clue in order to provide a first conclusion concerning the technical execution of two similar (but not identical) samples.

5 Conclusions

In this article, CW THz (0.1 THz) imaging applied both in reflection and in transmission mode was applied to two similar (but not identical) paintings on canvas. In particular, the first one (named sample A) reproduces exactly the famous artwork (an oil on canvas) of James Abbott McNeill Whistler, titled *Arrangement in Grey and Black, No. 1: Portrait of the Painter's Mother*, completed in 1871, while the second one is a good reproduction in which the nature and the texture of the canvas is very dissimilar with respect to the real one and the technical execution is slightly different. Although the

nature and the texture of the canvas can be observed from the rear side, one usually finds good reproductions in which the support is achieved with a bottom layer acting as a cover for the upper layers. Therefore, the inspection in reflection mode is important. In this case, the samples were prepared considering an identical final thickness, if compared to each other. The application of a cover layer on the rear side of sample B, identical to the canvas of sample A, improves the validity of the present method since also the transmission mode has been taken into account during the THz inspections. The polarization of the THz source used herein was also used in [71]. It was a priori considered, since anisotropic materials such as composites have a variable reflectance strictly connected to the fiber directions.

In real objects, the micro-sampling procedure and, therefore, the study of cross-sections can be considered as a second step to distinguish between artworks and forgeries. However, the micro-sampling procedure is, unfortunately, both micro-destructive and irreversible. Maybe the parameterization and analysis of various materials or the determination of the thickness influence on the THz and IRT results, can be considered a valid alternative. The micro-sampling procedure is obviously not applied on reproductions/copies of real artworks, and/or when the materials used in real artworks are well known/documented. It can be combined with imaging in order to discriminate between materials and/or attend to "determine a period of time" of execution for an object, by considering the palette of pigments used by the art master

(or by the forger). In addition, the use of the THz method combined with the use of the IRT method can help to provide information regarding the execution of the paint layers or the texture of the fabric used.

The THz results obtained in the transmission mode show different absorptivities for the textile supports, while thermographic results revealed both shallow and relatively deep anomalies in relation to the EOF (for PCT technique) or loading (for PLST technique) used. The PCT technique and THz method detect different signal variations. These signals variations can be attributed to sub-superficial anomalies than what it was possible to detect by the PLST technique. However, the PLST technique summarizes the most important noise linked to the use of a single lamp in the Loading 02. In addition, the consecutive images are strictly linked to the scanning of the depth. THz results are not immediately understandable to a non-expert in this matter, although when integrated with IRT results they can corroborate the main assumptions.

Although the THz is not new and the system used herein is a commercial product, the innovation is the use of the robot to scan the oil paintings, or more in general, the use of the robot in the cultural heritage field. It allows an in situ inspection when, e.g., it is not possible to move the artwork outside the museum due to microclimatic reasons. Our CW THz system has the advantage of operating via a simple experimental set up and is inexpensive, however, it cannot retrieve the defect depth. On the contrary, pulse THz system can assure quantitative analyses. Regarding the image processing, the intensity data are stored in a matrix in the CW THz system, which can be directly converted to a raster image. A perspective of the present work will be the use of the robot in combination with thermographic measurements, as well as the application of a pseudo-static reconstruction algorithm before the advanced image processing procedure. A short-wave IR camera (SWIR) can also be used both in reflection and in transmission modes considering both the semi-transparent nature of the object itself, and the possibility to perform a digital subtraction procedure between the reflectogram and the transmittogram with the aim of detecting the weaker areas of the canvas [60].

References

1. Abraham, E., Fukunaga, K.: Terahertz imaging applied to the examination of artistic objects. Stud. Conserv. **60**(6), 343–352 (2015)

2. Abraham, E., Younus, A., Delagnes, J.C., Mounaix, P.: Non-invasive investigation of art paintings by terahertz imaging. Appl. Phys. A **100**(3), 585–590 (2010)

3. Ahi, K., Anwar, M.: Developing terahertz imaging equation and enhancement of the resolution of terahertz images using deconvolution. In: Proc. SPIE 9856, Terahertz Physics, Devices, and Systems X: Advanced Applications in Industry and Defense, p. 98560N. International Society for Optics and Photonics (2016)

4. Ahi, K., Anwar, M.: Modeling of terahertz images based on x-ray images: a novel approach for verification of terahertz images and identification of objects with fine details beyond terahertz resolution. In: Proc. SPIE 9856, Terahertz Physics, Devices, and Systems X: Advanced Applications in Industry and Defense, p. 985610. International Society for Optics and Photonics (2016)

5. Ahi, K., Asadizanjani, N., Shahbazmohamadi, S., Tehranipoor, M., Anwar, M.: Terahertz characterization of electronic components and comparison of terahertz imaging with x-ray imaging techniques. In: Proc. SPIE 9483, Terahertz Physics, Devices, and Systems IX: Advanced Applications in Industry and Defense, p. 94830K. International Society for Optics and Photonics (2015)

6. Anderson, R., Koval, A.: James McNeill Whistler: Beyond the Myth. John Murray, London (1994)

7. Bein, B., Gibkes, J., Gu, J., Hüttner, R., Pelzl, J., Balageas, D., Déom, A.: Thermal wave characterization of plasma-facing materials by ir radiometry. J. Nucl. Mater. **191**, 315–319 (1992)

8. Bendada, A., Sfarra, S., Akhloufi, M., Caumes, J., Pradere, C., Batsale, J., Maldague, X., et al.: Subsurface imaging for panel paintings inspection: a comparative study of the ultraviolet, the visible, the infrared and the terahertz spectra. Opto Electron. Rev. **23**(1), 90–101 (2015)

9. Bendada, A., Sfarra, S., Genest, M., Paoletti, D., Rott, S., Talmy, E., Ibarra-Castanedo, C., Maldague, X.: How to reveal subsurface defects in kevlar® composite materials after an impact loading using infrared vision and optical ndt techniques? Eng. Fract. Mech. **108**, 195–208 (2013)

10. Bi, X., Krakowski, T., Weiser, D.: Integration of the silicon impatt diode in an analog technology (2014). US Patent App. 14/327,157

11. Craddock, P.: Scientific Investigation of Copies, Fakes and Forgeries. Routledge (2009)

12. Dandolo, C.L.K., Filtenborg, T., Skou-Hansen, J., Jepsen, P.U.: Analysis of a seventeenth-century panel painting by reflection terahertz time-domain imaging (thz-tdi): contribution of ultrafast optics to museum collections inspection. Appl. Phys. A **121**(3), 981–986 (2015)

13. Daniels, D.: Ground Penetrating Radar. Knoval (Institution of Engineering and Technology), New York (2004)

14. Dorment, R., MacDonald, M.: James mcneill whistler. The Art Book **2**(1), 15–16 (1995)

15. Duling, I., Zimdars, D.: Terahertz imaging: revealing hidden defects. Nat. Photon. **3**(11), 630–632 (2009)

16. Fernandes, H., Ibarra-Castanedo, C., Zhang, H., Maldague, X.: Thermographic non-destructive evaluation of carbon fiber-reinforced polymer plates after tensile testing. J. Nondestr. Eval. **34**(4), 1–10 (2015)

17. Fernandes, H., Zhang, H., Figueiredo, A., Ibarra-Castanedo, C., Guimarares, G., Maldague, X.: Carbon fiber composites inspection and defect characterization using active infrared thermography: numerical simulations and experimental results. Appl. Opt. **55**(34), D46–D53 (2016)

18. Fernandes, H., Zhang, H., Ibarra-Castanedo, C., Maldague, X.: Fiber orientation assessment on randomly-oriented strand composites by means of infrared thermography. Compos. Sci. Technol. **121**, 25–33 (2015)

19. Fernandes, H., Zhang, H., Maldague, X.: An active infrared thermography method for fiber orientation assessment of fiber-

reinforced composite materials. Infrared Phys. Technol. **72**, 286–292 (2015)

20. Fleming, G.H.: James Abbott McNeill Whistler: A Life. Windrush Press, Gloucestershire (1991)

21. Fukunaga, K., Ikari, T., Iwai, K.: Thz pulsed time-domain imaging of an oil canvas painting: a case study of a painting by pablo picasso. Appl. Phys. A **122**(2), 1–5 (2016)

22. Gallerano, G., Doria, A., Giovenale, E., Messina, G., Petralia, A., Spassovsky, I., Fukunaga, K., Hosako, I.: Thz-arte: non-invasive terahertz diagnostics for art conservation. In: Proceedings of the 33rd International Conference on Infrared, Millimeter and Terahertz Waves. IEEE (2008)

23. Gan, W.S.: Acoustical Imaging: Techniques and Applications for Engineers. Wiley, Chichester (2012)

24. Garbacz, P.: Terahertz imaging-principles, techniques, benefits, and limitations. Problemy Eksploatacji **1**, 81–92 (2016)

25. Gavrilov, D., Maev, R.G., Almond, D.: A review of imaging methods in analysis of works of art: thermographic imaging method in art analysis. Can. J. Phys. **92**(4), 341–364 (2014)

26. Groves, R., Pradarutti, B., Kouloumpi, E., Osten, W., Notni, G.: 2d and 3d non-destructive evaluation of a wooden panel painting using shearography and terahertz imaging. Ndt & E Int. **42**(6), 543–549 (2009)

27. Hartwick, T., Hodges, D., Barker, D., Foote, F.: Far infrared imagery. Appl. Opt. **15**(8), 1919–1922 (1976)

28. Hartwick, T.S.: Far infrared imaging techniques for law enforcement applications. In: Proc. SPIE 0108, Optics in Security and Law Enforcement I, pp. 139–140. International Society for Optics and Photonics (1977)

29. Ibarra-Castanedo, C.: Quantitative subsurface defect evaluation by pulsed phase thermography: depth retrieval with the phase. Ph.D. thesis, Université Laval (2005)

30. Ibarra-Castanedo, C., Maldague, X.P.: Infrared thermography. In: Czichos, H. (ed.) Handbook of Technical Diagnostics, pp. 175–220. Springer, Berlin (2013)

31. Ibarra-Castanedo, C., Sfarra, S., Ambrosini, D., Paoletti, D., Bendada, A., Maldague, X.: Subsurface defect characterization in artworks by quantitative pulsed phase thermography and holographic interferometry. Quant. InfraRed Thermogr. J. **5**(2), 131–149 (2008)

32. Ibarra-Castanedo, C., Sfarra, S., Ambrosini, D., Paoletti, D., Bendada, A., Maldague, X.: Diagnostics of panel paintings using holographic interferometry and pulsed thermography. Quant. InfraRed Thermogr. J. **7**(1), 85–114 (2010)

33. Karpowicz, N., Zhong, H., Xu, J., Lin, K.I., Hwang, J.S., Zhang, X.: Comparison between pulsed terahertz time-domain imaging and continuous wave terahertz imaging. Semicond. Sci. Technol. **20**(7), S293–S299 (2005)

34. Kasap, S.O.: Principles of Electronic Materials and Devices. McGraw-Hill, New York (2006)

35. Koch, M., Hunsche, S., Schumacher, P., Nuss, M., Feldmann, J., Fromm, J.: Thz-imaging: a new method for density mapping of wood. Wood Sci. Technol. **32**(6), 421–427 (1998)

36. Koch Dandolo, C.L., Cosentino, A., Jepsen, P.U.: Inspection of panel paintings beneath gilded finishes using terahertz time-domain imaging. Stud. Conserv. **60**(S1), S159–S166 (2015)

37. Kühn, H.: Trace elements in white lead and their determination by emission spectrum and neutron activation analysis. Stud. Conserv. **11**(4), 163–169 (1966)

38. Kukushkin, I., Muravev, V., Tsydynzhapov, G., Fortunatov, A.: High-speed giga-terahertz imaging device and method (2011). US Patent App. 13/336,912

39. Labaune, J., Jackson, J., Pages-Camagna, S., Duling, I., Menu, M., Mourou, G.: Papyrus imaging with terahertz time domain spectroscopy. Appl. Phys. A **100**(3), 607–612 (2010)

40. Lewis, R.A.: Terahertz Physics. Cambridge University Press, Cambridge (2012)

41. Liu, B., Zhang, H., Fernandes, H., Maldague, X.: Quantitative evaluation of pulsed thermography, lock-in thermography and vibrothermography on foreign object defect (fod) in cfrp. Sensors **16**(5), 743 (2016)

42. Lizarraga, J., Del-Rio, C.: Resolution capabilities of future thz cameras. In: Proceedings of the 4th European Conference on Antennas and Propagation. IEEE (2010)

43. Lopez, F., Ibarra-Castanedo, C., de Paulo Nicolau, V., Maldague, X.: Optimization of pulsed thermography inspection by partial least-squares regression. NDT & E Int. **66**, 128–138 (2014)

44. Maev, R.G., Green Jr., R., Siddiolo, A.: Review of advanced acoustical imaging techniques for nondestructive evaluation of art objects. Res. Nondestruct. Eval. **17**(4), 191–204 (2006)

45. Maldague, X.: Theory and Practice of Infrared Technology for Nondestructive Testing. Wiley, New York (2001)

46. Malykh, N., Nagornyi, A., Yampolskii, E.: Submillimeter-wave imagery. Instrum. Exp. Tech. **18**(1), 182–184 (1975)

47. Murray, A., Mecklenburg, M.F., Fortunko, C., Green, R.E.: Air-coupled ultrasonic system: a new technology for detecting flaws in paintings on wooden panels. J. Am. Inst. Conserv. **35**(2), 145–162 (1996)

48. Naftaly, M., Miles, R.: Terahertz time-domain spectroscopy of silicate glasses and the relationship to material properties. J. Appl. Phys. **102**(4), 043517 (2007)

49. Nguyen, D.T.: Design, modeling, and characterization of innovative terahertz detectors. Ph.D. thesis, Université de Grenoble (2012)

50. Oyama, Y., Zhen, L., Tanabe, T., Kagaya, M.: Sub-terahertz imaging of defects in building blocks. NDT & E Int. **42**(1), 28–33 (2009)

51. Picollo, M., Fukunaga, K., Labaune, J.: Obtaining noninvasive stratigraphic details of panel paintings using terahertz time domain spectroscopy imaging system. J. Cult. Herit. **16**(1), 73–80 (2015)

52. Pieraccini, M., Mecatti, D., Fratini, M., Atzeni, C., Seracini, M.: A high frequency gpr application to the cultural heritage survey: the search of the" battle of anghiari" by leonardo da vinci. In: Proceedings of the 10th International Conference on Grounds Penetrating Radar, vol. 1, pp. 391–394. IEEE (2004)

53. Rajic, N.: Principal component thermography for flaw contrast enhancement and flaw depth characterisation in composite structures. Compos. Struct. **58**(4), 521–528 (2002)

54. Rostami, A., Rasooli, H., Baghban, H.: Terahertz Technology: Fundamentals and Applications. Springer, Berlin (2011)

55. Schlömann, E.: Dielectric losses in ionic crystals with disordered charge distributions. Phys. Rev. **135**(2A), A413–A419 (1964)

56. Sfarra, S., Bendada, A., Ibarra-Castanedo, C., Ambrosini, D., Paoletti, D., Maldague, X.: Santa maria di collemaggio church (l'aquila, italy): historical reconstruction by non-destructive testing techniques. Int. J. Archit. Herit. **9**(4), 367–390 (2015)

57. Sfarra, S., Ibarra-Castanedo, C., Ambrosini, D., Paoletti, D., Bendada, A., Maldague, X.: Discovering the defects in paintings using non-destructive testing (ndt) techniques and passing through measurements of deformation. J. Nondestruct. Eval. **33**(3), 358–383 (2014)

58. Sfarra, S., Ibarra-Castanedo, C., Paoletti, D., Maldague, X.: Infrared vision inspection of cultural heritage objects from the city of l'aquila, italy and its surroundings. Mater. Eval. **71**(5), 561–570 (2013)

59. Sfarra, S., Ibarra-Castanedo, C., Ridolfi, S., Cerichelli, G., Ambrosini, D., Paoletti, D., Maldague, X.: Holographic interferometry (hi), infrared vision and x-ray fluorescence (xrf) spectroscopy for the assessment of painted wooden statues: a new integrated approach. Appl. Phys. A **115**(3), 1041–1056 (2014)

60. Sfarra, S., Ibarra-Castanedo, C., Santulli, C., Paoletti, D., Maldague, X.: Monitoring of jute/hemp fiber hybrid laminates by nondestructive testing techniques. Sci. Eng. Compos. Mater. **23**(3), 283–300 (2016)

61. Sfarra, S., Ibarra-Castanedo, C., Tortora, M., Arrizza, L., Cerichelli, G., Nardi, I., Maldague, X.: Diagnostics of wall paintings: a smart and reliable approach. J. Cult. Herit. **18**, 229–241 (2016)

62. Sfarra, S., Perilli, S., Paoletti, D., Ambrosini, D.: Ceramics and defects. J. Therm. Anal. Calorim. **123**(1), 43–62 (2016)

63. Sfarra, S., Theodorakeas, P., Černeckỳ, J., Pivarčiová, E., Perilli, S., Koui, M.: Inspecting marquetries at different wavelengths: the preliminary numerical approach as aid for a wide-range of non-destructive tests. J. Nondestruct. Eval. **36**(1), 6 (2017)

64. Siddiolo, A., Maeva, A., Maev, R.G.: Air-coupled imaging method applied to the study and conservation of paintings. In: Acoustical Imaging, vol. 28, pp. 3–12. Springer (2007)

65. Siebert, K.J., Löffler, T., Quast, H., Thomson, M., Bauer, T., Leonhardt, R., Czasch, S., Roskos, H.G.: All-optoelectronic continuous wave thz imaging for biomedical applications. Phys. Med. Biol. **47**(21), 3743–3748 (2002)

66. Strom, U., Taylor, P.: Temperature and frequency dependences of the far-infrared and microwave optical absorption in amorphous materials. Phys. Rev. B **16**(12), 5512–5522 (1977)

67. Stubbs, B.A.: James McNeill Whistler: A Biographical Outline, vol. 1. Freer Gallery of Art, Washington (1950)

68. Tortora, M., Sfarra, S., Chiarini, M., Daniele, V., Taglieri, G., Cerichelli, G.: Non-destructive and micro-invasive testing techniques for characterizing materials, structures and restoration problems in mural paintings. Appl. Surf. Sci. **387**, 971–985 (2016)

69. Trafela, T., Mizuno, M., Fukunaga, K., Strlič, M.: Quantitative characterisation of historic paper using thz spectroscopy and multivariate data analysis. Appl. Phys. A **111**(1), 83–90 (2013)

70. Wittstruck, R.H.: Method for high frequency device operation with high temperature and radiation hard characteristics (1997). US Patent 5,652,551

71. Xiao, X., Leung, H.M., Chan, C.T., Wen, W.: Manipulation of the polarization of terahertz wave in subwavelength regime. Sci. Rep. **5** (2015)

72. Yousefi, B., Fleuret, J., Zhang, H., Maldague, X.P., Watt, R., Klein, M.: Automated assessment and tracking of human body thermal variations using unsupervised clustering. Appl. Opt. **55**(34), D162–D172 (2016)

73. Zhang, H., Fernandes, H., Dizeu, F.B.D., Hassler, U., Fleuret, J., Genest, M., Ibarra-Castanedo, C., Robitaille, F., Joncas, S., Maldague, X.: Pulsed micro-laser line thermography on submillimeter porosity in carbon fiber reinforced polymer composites: experimental and numerical analyses for the capability of detection. Appl. Opt. **55**(34), D1–D10 (2016)

74. Zhang, H., Fernandes, H., Hassler, U., Ibarra-Castanedo, C., Genest, M., Robitaille, F., Joncas, S., Maldague, X.: Comparative study of microlaser excitation thermography and microultrasonic excitation thermography on submillimeter porosity in carbon fiber reinforced polymer composites. Opt. Eng. **56**(4), 041304 (2017)

75. Zhang, H., Hassler, U., Genest, M., Fernandes, H., Robitaille, F., Ibarra-Castanedo, C., Joncas, S., Maldague, X.: Comparative study on submillimeter flaws in stitched t-joint carbon fiber reinforced polymer by infrared thermography, microcomputed tomography, ultrasonic c-scan and microscopic inspection. Opt. Eng. **54**(10), 104109 (2015)

76. Zhang, H., Yu, L., Hassler, U., Fernandes, H., Genest, M., Robitaille, F., Joncas, S., Holub, W., Sheng, Y., Maldague, X.: An experimental and analytical study of micro-laser line thermography on micro-sized flaws in stitched carbon fiber reinforced polymer composites. Compos. Sci. Technol. **126**, 17–26 (2016)